Anomalous diffusion for molecules under confinement: Thermal resistance effect

Abstract

It is common knowledge that the higher the temperature, the faster the diffusion. In this work, a novel counterintuitive diffusion that the movement of long-chain molecules slow down as the temperature increase under confinement has been observed. The report manifests this anomalous diffusion caused by the "thermal resistance effect", where the diffusion resistance of linear-chain molecule is equivalent to that of the branched-chain configuration at high temperature, and then restrains the process of transportation in the nanoscale channels. This work enriches the anomalous diffusion phenomenon and provides fundamental insights for the novel diffusion mechanism inside confined systems.

Significance Statement

Diffusion represents the primary process in practical multidisciplinary areas, such as separation and catalysis. Generally speaking, the diffusion is positively correlated with temperature for the contribution of the thermal motion. For the first time, the anomalous phenomenon that the higher the temperature, the slower the diffusion has been observed for the linear-chain hydrocarbon molecule under confinement. Such obstruction in self-diffusion coefficients is resulted by the novel mechanism of "thermal resistance effect", where the configuration of guest molecule is significantly deformed with temperature effect and then strongly restrains the process of transportation in nanoscale channels at high temperature.

Main Text

Introduction

Molecules or atoms are subject to permanent random movement as a consequence of their thermal energy in the condensed phase, which is referred to as Brownian motion. The diffusion process, is a universal phenomenon that occurs, on different time scales, in all states of matter [1]. It is critically important in the separation and catalytic processes involving the application of nanoporous materials [2-5].

Besides the condensed phase, the diffusion in the confined space of channels at nano-scale (*i.e.*, less than 1 nm) has spurred significant interesting recently [5]. Among lots of nanoporous materials, zeolite with regular crystalline shapes and wide variety of topologies are best known, not only due to their widely used in industrial applications, but also widely studied in microscale [3]. An intriguing case of molecules movement inside zeolite is called "single-file diffusion", which only takes place in one-dimensional (1-D) channels where the molecules cannot pass each other and a dramatic decrease in mobility of the molecules could be observed [6]. Single-file diffusion has been found in lots of materials with 1-D channels and has been detected by NMR experiment [7-9]. Ghorai *et al.* found the "levitation effect" for the maximum self-diffusivity of a molecule whose diameter is close to the pore size of zeolite [10] and Nag *et al.* illustrated the efficacy of the levitation effect for separating real mixtures of both linear n-pentane and its branched isomer [11]. Some other interesting effect like incommensurate diffusion [12, 13], molecular traffic control [14], resonance diffusion [15, 16], window effect [17] and molecular path control [18] are well known. It is evident that anomalous diffusion is still being discovered and continues to be an exciting field of research with a bounty of surprise.

For all the diffusion behavior (*i.e.*, normal and anomalous described above), the transport of sorbate is influenced by the factors of temperature. Generally, the diffusivity and temperature follows the Arrhenius equation (Equation 1), and thus the higher temperature, the faster diffusion behavior is [19-20].

$$D_s = D_0 e^{\frac{-Ea}{RT}} \qquad (1)$$

In which D_s represents the self-diffusion coefficient, D_0 is a pre-exponential factor, E_a stands for the diffusion activation energy, R and T respectively represent molar gas constant and temperature. For instance, Ghysels *et al.* expressed that diffusion coefficients (D_s) of ethene in several zeolites show the monotone increasing tendency as temperature [21]. Gao *et. al* measured the diffusion coefficients of different alkane at different temperature in various zeolites by pulsed field gradient nuclear magnetic resonance (PFG-NMR) and found that they follow Equation 1 as well. In this work, an anomalous effect for long-chain molecules (*i.e.* alkane and alkene (seen in Table S2)) inside MFI zeolite was observed for the first time, where the diffusion coefficient was slowed down with the increasing temperature for n-dodecane (C12) molecules (see Figure 1(b)). On the basis of molecular dynamics (MD) simulation, the connection between the structure and

anomalous diffusion has been established, which provide fundamental insights for the diffusion property inside confined channels.

Results

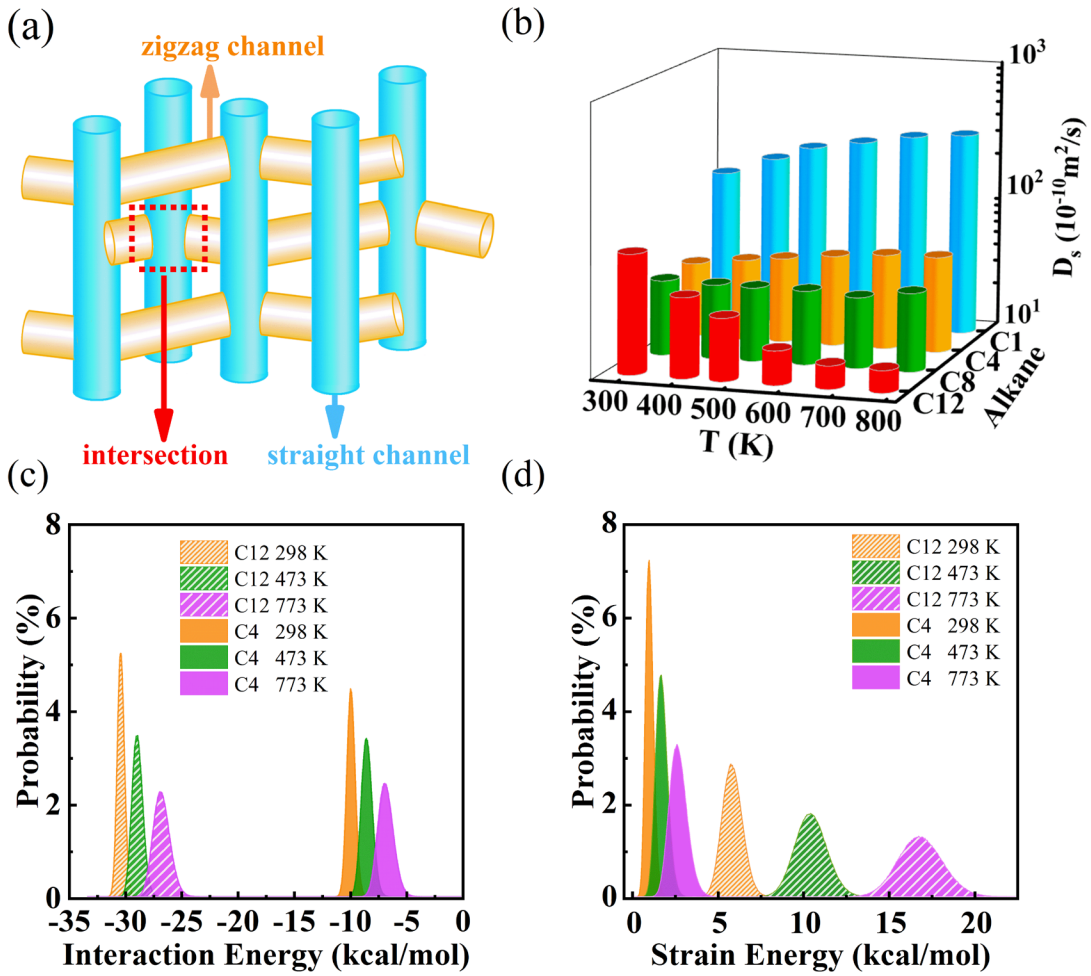

Figure 1. (a) 3-D channels of MFI zeolite, the blue and orange cylinders represent the straight and zigzag channels, respectively. (b) Self-diffusion coefficients of methane (C1), *n*-butane (C4), *n*-octane (C8) and *n*-dodecane (C12) in MFI zeolite at different temperature. (c) Distributions of interaction energy between molecules and MFI zeolite, and (d) distributions of strain energy for alkane molecules (*n*-butane (C4) and *n*-dodecane (C12)) at 298, 473 and 773 K.

The diffusion behaviors of molecules inside the confined channel are strongly correlated with the framework of zeolite. Figure 1(a) shows the 3-dimensional channels (3-D) of MFI, which possess 10-ring zigzag channels with a window size of 5.1 Å × 5.5 Å along the X and Z direction, as well as 10-ring straight channel (5.3 Å × 5.6 Å) distributed in the Y direction (see Fig. S1(a)). As is well known that self-diffusion coefficient (D_s) could quantitatively describe the movement of guest molecules inside confined channels [22]. In this work, D_s of linear alkane molecules (*i.e.* methane (C1), *n*-butane (C4), *n*-octane(C8) and *n*-dodecane (C12), which are the main component of natural gas, gasoline as well as diesel and widely investigated in the field of petrochemical-industry [23]) in the zeolite catalysis, have been explored. It shows that D_s are in agreement with Jobic's work which are on the order from 10^{-9} to 10^{-8} m^2/s [24, 25]. As shown in Table S1, the simulated D_s of

methane at 473 K is *ca.* 2.21 × 10^{-8} m^2/s, which is almost the same as experimental result (2.05 × 10^{-8} m^2/s) detected by quasi-elastic neutron scattering (QENS) at the same temperature [24]. As for C4 at ambient temperature, our result (0.35 × 10^{-8} m^2/s) is also on the same order of Leroy and coworkers' work (0.41 × 10^{-8} m^2/s) [26]. In addition, Runnebaum and co-workers reported D_s of C12 in zeolite MFI at 400 K (*ca.* 0.40 × 10^{-8} m^2/s) [16], and thus further confirmed our calculations (0.38× 10^{-8} m^2/s).

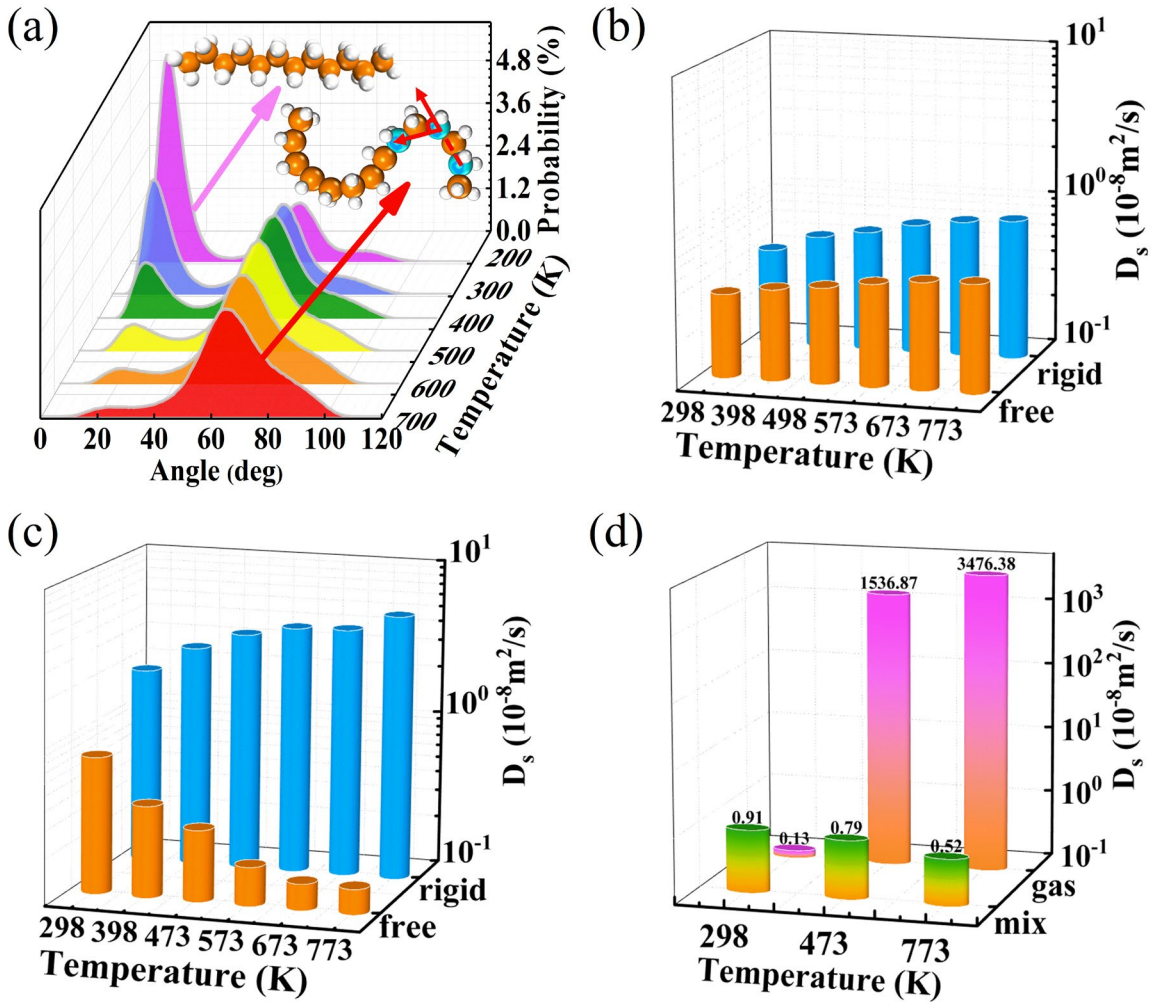

Figure 2. (a) Distributions of distorted angle for n-dodecane at various temperature. (b) Self-diffusion coefficient (D_s) of rigid C4 (linear-C4, blue histogram), and free C4 (flexible C4, orange histogram). (c) The self-diffusion coefficient (D_s) of rigid C12 (linear-C12, blue histogram), and free C12 (flexible C12, orange histogram). (d) D_s of mixture for rigid linear-C12/branched-C12 (Green orange gradient histogram) inside MFI and at condensed (gas) phase (pink orange gradient histogram) at 298, 473 and 773 K.

According to Equ. (1), D_s of linear alkane molecules is strongly dependent on the temperature. As illustrated in Figure 1(b), for the short-chain alkane molecules (*i.e.* C1 and C4), the diffusion is positively correlated with temperature due to the higher temperature increased thermal movement. However, in contrast to short-chain alkane, there is no monotonic increasing of D_s as temperature for long-chain paraffin (*e.g.*, C8 and C12). In particular for C12, a counterintuitive diffusion behavior was determined that the movement of molecule has slowed down as the temperature increases.

It's observed that D_s is 1.01×10^{-8} m^2/s at 298 K, while it inversely decreases to 0.30×10^{-8} and 0.17×10^{-8} m^2/s at 573 K and 773 K, respectively (see Table S1). It should be noted that it was the first time to observe such anomalous diffusion as the temperature variations inside zeolite.

It is well-known that the diffusion behaviors are closely related to the interaction between adsorbate and zeolite framework [20]. And thus, the interaction energy and strain energy (configuration energy) of C4 and C12 were investigated to understand the anomalous diffusion. As is visualized in Figure 1(c), the interaction energy within zeolite for C12 is *ca.* 3 times stronger than that for C4 due to its longer chain. However, there was no significant variance on this quantity for both C4 and C12 at different temperature, which indicates the interaction energy may not be the main factor that induces the anomalous diffusion. However, for the strain energy, it is within 5 kcal/mol with the variation of temperature for C4, but it is significantly increased from 6 kcal/mol (298 K) to 17 kcal/mol (773 K) for C12 (see Figure 1(d)). The larger strain energy clearly indicated the severely structural distortion for C12 at relatively high temperature.

The structural distortion was also quantitatively confirmed by the intramolecular bending angle of the molecule. As shown in Figure 2(a) and Figure S2, the number of bending molecules increases with increasing temperature, such as 40% of C12 with the intramolecular C-C-C angle are distorted by larger than 45° at 298 K, while almost 90% larger than 45° under 773 K, which confirmed its pronounced deformation again. And thus, the anomalous diffusion may be caused by the structure deformation of the long-chain paraffin.

In order to further determine the effect of the molecular deformation with the increasing temperature on the anomalous diffusion in ZSM-5 zeolite, a theoretical simulation on the basis of model only contains fixed structure without any structural deformation (as rigid molecule) for C4 and C12 has been investigated. As shown in Figure 2(b), for short chain alkane like C4, it shows that structural distortion contributes to diffusion deceleration. For instance, D_s of C4 are 0.43×10^{-8}, 0.61×10^{-8} and 0.81×10^{-8} m^2/s at 298, 473 and 773 K, respectively, which are slightly larger than the according flexible model (i.e., 0.35×10^{-8} (298 K), 0.42×10^{-8} (473 K), 0.51×10^{-8} (773 K) m^2/s). It is obvious that even for the short chain C4, the molecular bending inside the zeolite confined space could hinder the mass transfer but still maintain a positively correlation for the significant contribution of the kinetic energy for high temperature. In contrast to that of C4, D_s *of* C12 with rigid and flexible construction possessed an antipodal temperature dependence. Figure 2(c) clearly indicates that the anomalous diffusion has been disappeared and presented a positive relationship between D_s and temperature when the rigid C12 is applied. For example, the self-diffusion coefficients of rigid C12 molecules are 1.83×10^{-8} (298 K), 3.45×10^{-8} (473 K) and 5.18×10^{-8} m^2/s (773 K).

In addition, a controllable simulation of a mixture of rigid linear C12 and rigid branched C12 both without deformation was applied to check the effect of concentration of branched-chain component (*i.e.*, $M_{n\text{-}C12}/M_{branched\text{-}C12}$) on the diffusion properties. According to MD simulation, the relative ratios of $M_{linear\text{-}C12}/M_{branched\text{-}C12}$ were varied with the temperature (*e.g.*, 8:4, 4:8, 2:10 at 298 K, 473 K, and 773 K). Interestingly, it shows that the diffusion coefficients are indeed reduced as temperature increased (see Figure 2(d)), which is in agreement with the trend of realistic simulation for flexible n-dodecane (C12) in MFI zeolite (see Figure 1(b)), suggesting that the significant diffusion resistance of linear-chain molecules is due to the presence of branched-chain-like configurations at high temperature.

Quantitatively comparison of molecular deformation at different temperature will further illustrate the anomalous effect at varied temperature. The root-mean-square deviation (RMSD) of Cartesian positions is a standard parameter to evaluate the molecular deformation in the confined zeolite (see Table. S3) [27]. As is depicted in Figure 3(a), the RMSD of C4 is less than 1.0 Å even at 773 K, and the two peaks at 0.5 and 1 Å are regarded as the two adsorbed states inside the straight (smaller distortion) and zigzag (greater distortion) channels, consistent with the results mentioned above, the molecular deformation increases gradually as the temperature increases that

the peak at 1 Å enhances with the peak at 0.5 Å educes. This is reason for the strain energy increases as the temperature goes up. While for C12, a new peak at 2.0 Å was observed at 773 K (see Figure 3(a)), which means that long chain molecule is dramatically distorted at higher temperature. Furthermore, a wide distribution of RMSD of C12 with high temperature is apparently illustrated that linear structure of C12 at low temperature was gradually undermined, and a more significant deformation was present at a higher temperature, and consequently lead to the anomalous diffusion.

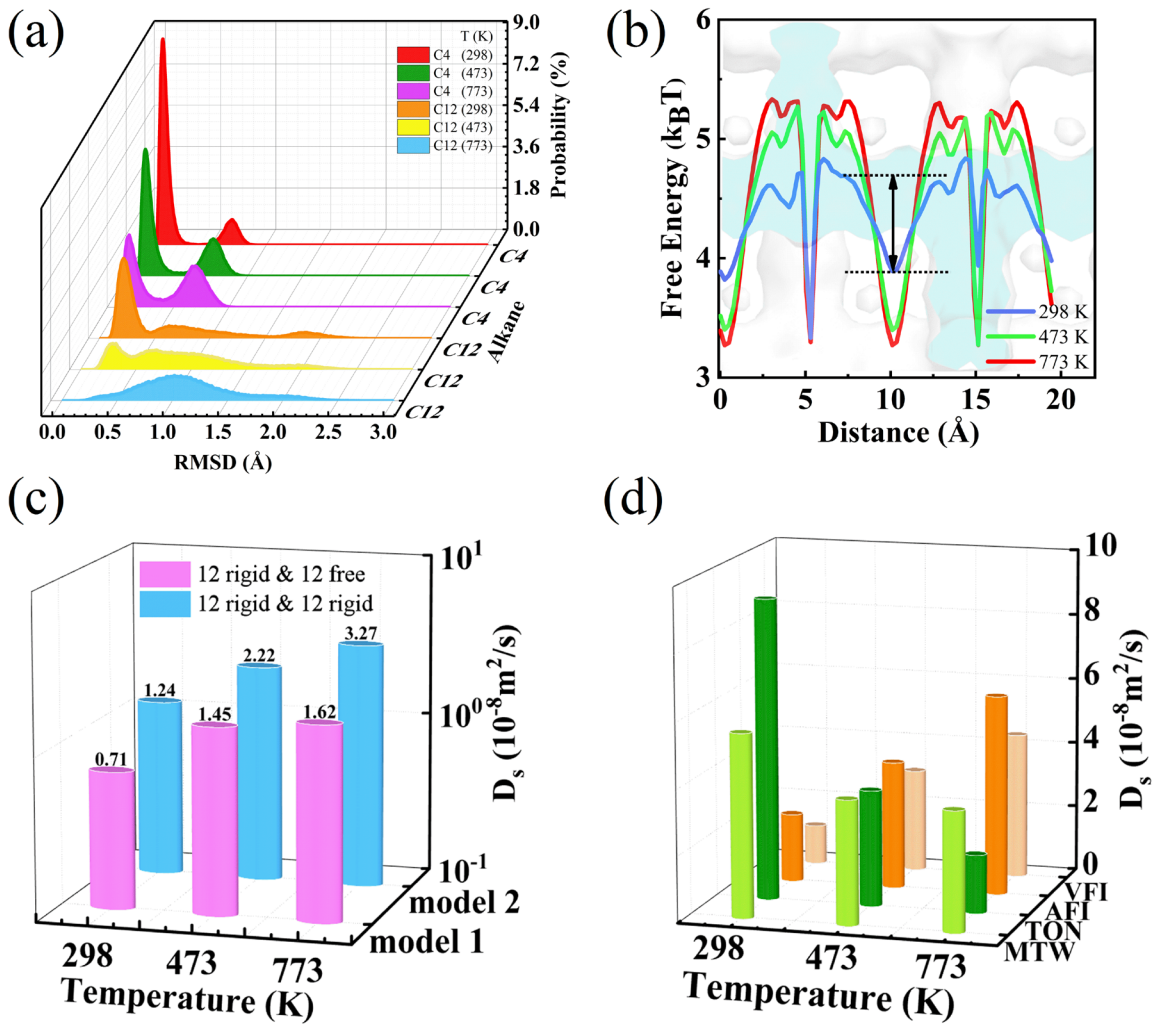

Figure 3. (a) The root-mean-square deviation (RMSD) of C4 and C12 molecule inside MFI zeolite. (b) The free energy of C12 diffuse inside MFI zeolite. (c) Diffusion coefficient of rigid C12 coexist flexible (blue histogram) and rigid C12 (pink histogram). (d) Diffusion coefficient of C12 inside MTW, TON, AFI and VFI zeolites.

It's illustrated that the energy barrier provide the directly information about the diffusion process. To further illustrate this point, free energy profiles (ΔG) of C4 and C12 inside MFI zeolite with varied temperature were performed. Figure 3(b) illustrated that the higher temperature, the larger diffusion energy barrier was for C12. For example, ΔG was 0.8 k_BT at 298 K, while it dramatically increased

to 1.6 k_BT and 2.0 k_BT at 473 K and 773 K, respectively. Therefore, the diffusion was strongly hindered at high temperature for C12 from the view of the energy barrier, as well as a negative correlation was present between diffusion coefficient and temperature. While for C4, a completely different trend was observed that two local minima energy is located in the intersection, for the length of C4 is much shorter to appear at the intersection (See Fig. S3).

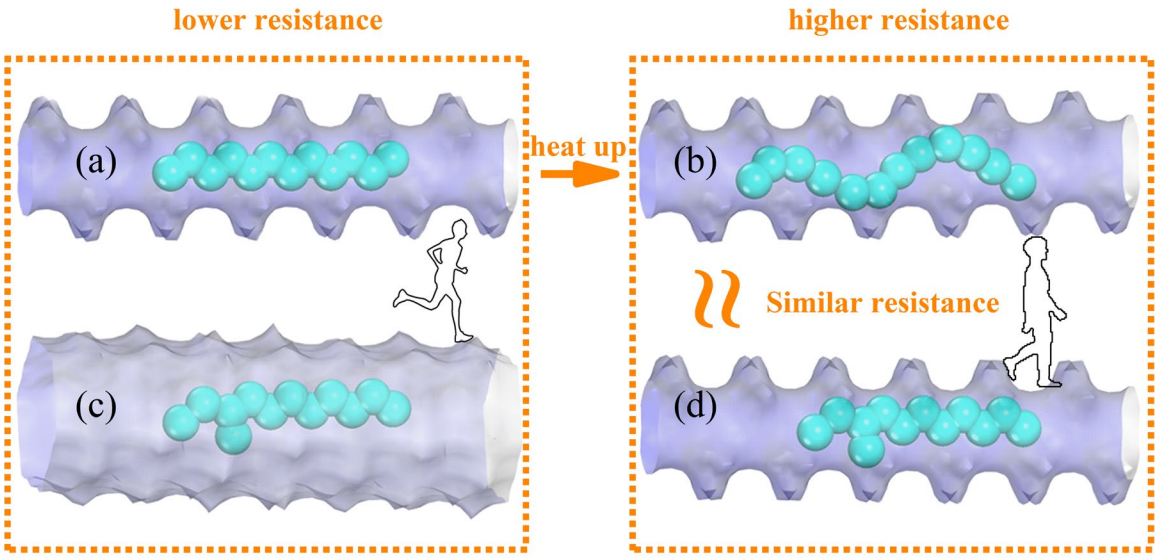

Figure 4. The structure of C12 molecule diffuse inside confined channel at (a) 298 K and (b) 773 K in MTW zeolite (small pore size). Diffusion of branched-chain C12 inside channels of (c) VFI (large pore size) and (d) MTW.

As is well known that thermistor is a kind of temperature sensitive component, and the thermistor with positive temperature coefficient owns a larger resistance under the higher temperature [29]. Interestingly, this anomalous behavior shows the similar property to thermistor and thus can be named as "thermal resistance effect" (TRE) in the diffusion process, where the temperature could lead to the decrease diffusion coefficient of C12 due to the structure distortion of long-chain alkane (see Figure. 2(a) and Figure 4(b)). Furthermore, it is interestingly found that bending molecule not only block the diffusion of the induced-bulky configuration themselves, but also strongly obstruct the movement of the other linear component during the diffusion process (as shown in Figure 3(c)). Two models were simulated to verify this viewpoint. Model 1, a system with 12 rigid coexisted 12 flexible molecule C12. Model 2, and another comparative system with 12 rigid coexisted 12 rigid molecule C12 were applied. D_s of 12 rigid molecule of both systems is calculated for the determination of how the flexible and rigid molecule affect the diffusion of other structures. It obviously manifests that the former system owns flexible skeleton possess a smaller D_s (for model 1, D_s is 0.71×10^{-8} (298 K), 1.45×10^{-8} (473 K), 1.62×10^{-8} (773 K) m^2/s) than the latter one (model 2, 1.24×10^{-8} (298 K), 2.22×10^{-8} (473 K), 3.27×10^{-8} (773 K) m^2/s) exclusively owns rigid configuration. Furthermore, a marginal difference of D_s between the two systems at low temperature is exhibited (0.53×10^{-8} m^2/s at 298 K), while as the temperature increases, the difference significantly became more obvious (1.65×10^{-8} m^2/s at 773 K). It's indicated that more linear-chain molecules have been

present in the branched-like configuration at higher temperature, and consequently slow down the diffusion. In general, two kinds of TRE for the deformed molecule have been observed in MFI zeolite during the diffusion process, including hinder the diffusion of themselves, (Figure 2(b) and 2(c)), as well as restrain the diffusion of other molecules co-adsorbed in the zeolite channels (Figure 3(c)).

It's noteworthy that the temperature-induced deformation of the molecule is general trends for the gas molecule. However, there is no TRE to be observed in the condensed phase even for the distorted (Fig.S4(d)) at high temperature (Table. S2 and Figure 2(d)). Apparently, TRE is strongly correlated to the zeolite framework and its pore size. Therefore, we discussed the existence conditions of TRE of the diffusion in the zeolite systems. MTW, TON, AFI and VFI are 1-D channel zeolite with the pore size of 5.6 Å × 6.0 Å, 4.6 Å × 5.7 Å, 7.3 Å × 7.3 Å and 12.7 Å ×12.7 Å, respectively (see Fig. S1(b) and S1(c)). It illustrated that the TRE diffusion would only present in MTW and TON zeolite (see Figure 3(d) and Table. S2), whose pore size is similar to that of MFI. While a normal behavior was obtained in larger channel of AFI and VFI zeolite due to the weaker host/guest interaction between distorted C12 and framework at high temperature (see Fig. S4 and Figure 4-5). Furthermore, the confinement effect in zeolite can be qualitatively assessed by the scatter plot of the reduced density gradient (RDG) in real space, which is an effective and widely used tool to visualize non-covalent interaction between adsorbates and zeolite. The RDG scatters of the *n*-C12 in MFI, MTW and VFI at 298 K and 773 K were illustrated in Figure 5. The gradient isosurfaces (s = 0.5 a.u.) are colored on a blue-green-red scale according to values of the electron density multiplied by the sign of the second Hessian eigenvalue ($\mathrm{sign}(\lambda_2)\rho$), ranging from -0.035 to 0.02 a.u. Blue indicates strong attractive interaction, green indicates weak attractive interaction, and red indicates strong repulsive interaction [28]. Obviously, there are almost no hydrogen-bonding interaction and strong repulsive interaction between C12 and three zeolite frameworks ((no spike is observed in the rigion colored blue and red) see method in SI for a detailed description) but the van der Waals (vdW) interactions (for the low-density, low-gradient spike now lying at green rigion) reveal the different tendencies. For example, dodecane inside MFI and MTW at higher temperature owns a rigion with higher density than that at lower tempeature (Figure 5), which indicates the stronger interaction between C12 and MFI(or MTW) at high temperature. While, the density of the spikes of VFI is almost the same at both of the low and high temperature, which clearly illustrated that the the variations of the temperature will lead very slightly change to the interactions. On the other hand, the less concentrated distribution of the RDG than those of MFI

and MTW demonstrated a less confinement effect of C12 inside VFI zeolite channel with large poresize, regardless of the degree of dodecane deformation with the temperature.

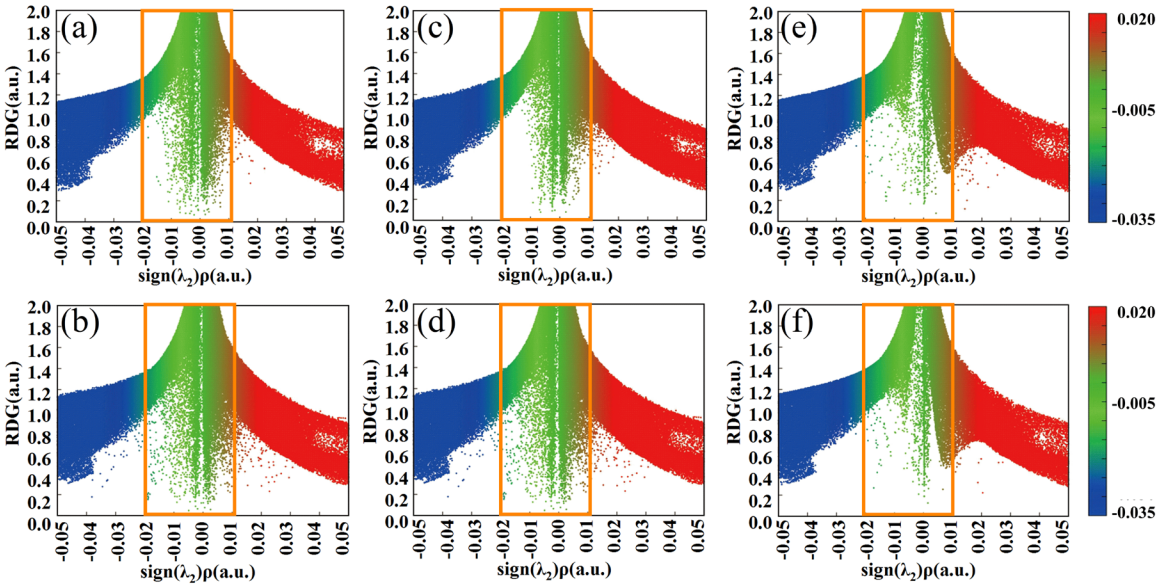

Figure 5. The RDG scatter of dodecane in MFI (left), MTW (middle) and VFI (right) at 298 K (upper) and 773 K (bottom). The embedded structures are used to calculated RDG.

Furthermore, we also consider the effect of concentration (see Supplemental Material Fig. S5) as well as other long chain molecule such as cetane and dodecatylene (Table S2), it was found the anomalous diffusion also presented for other long chain hydrocarbon as well as under a higher concentration, suggesting the robust of the TRE. Over all, the confinement effect of zeolite channels as well as high temperature induced the distortion of long-chain molecules will breed thermal resistance effect.

Discussion

In summary, an anomalous effect for molecules diffusion dependent on temperature was observed that the higher temperature would induce the smaller diffusion coefficient of long-chain molecules (*e.g.*, C12 and other longer chains hydrocarbon molecules) inside the confined channel of zeolite. Notably, such counterintuitive effect originates from the deformation of adsorbate as well as the increased confinement (*i.e.*, host/guest interaction) result by the relatively bulky-size under the higher temperature in the zeolite channels. Similar to the thermistor, it is a novel "thermal resistance effect" in the diffusion behavior inside zeolite confined channels. This work will enrich anomalous mechanism of the diffusion phenomenon, and could shed new lights toward fundamental understanding of diffusion process.

Materials and Methods

Molecular dynamics simulation

In our simulations, the initial structure of MFI, MTW, TON, AFI and VFI were taken from the International zeolite Associations (IZA) database (see Fig. S1) [29] and optimized by GULP [30] with SLC core-shell force field [31-32]. A 2 × 2 × 3 supercell with the loading of 12 molecules (C4, C8, C12) was used for MFI, while larger 3 × 3 × 4 supercell of MFI was performed for CH_4 (36 molecules) to avoid large fluctuations in temperature. The 2 × 10 × 4, 2 × 2 × 6, 3 × 3 × 5 and 3 × 3 × 6 supercell with the loading of 16, 8, 9 and 9 $C_{12}H_{26}$ (n-dodecane) molecules were used for MTW, TON, AFI and VFI, respectively. Molecular dynamics (MD) simulations were performed in the canonical ensemble (NVT), where the number of particles (N), volume (V), and temperature (T) were kept constant. The simulated temperature was ranging from 298 K to 773 K (i.e. 298, 398, 473, 573, 673 and 773 K) and controlled by a Nosé-Hoover thermostat with a coupling time constant of 0.1 ps. For the molecules in condensed phase, NPT ensemble (constant number of particles N, pressure P, and temperature T) was used for equilibration so that the volumes were stable at the pressure of 1 atm and various temperature, then NVT ensemble was carried out for studying the diffusion behaviors. The leapfrog Verlet algorithm was used to integrate the Newton's equations of motion with a time step of 0.5 fs. The TraPPE-zeo [33] and TraPPE-UA [34] force field were used for zeolite and hydrocarbon, respectively. All the Lennard–Jones cross-interaction parameters were determined by the Lorentz–Berthelot mixing rules, and the cutoff radius was 14 Å. Each MD simulation was equilibrated for 2×10^6 steps, and then, 4×10^7 steps production was recorded for the research on the diffusion behaviors of adsorbate molecules. The trajectories were recorded every 1000 steps, and 3 independent MD simulations were carried out for better statistics. All MD simulations were performed in the DL_POLY 2.0 code [35].

Diffusion coefficient

In this work, the mean square displacement (MSD) of adsorbates is defined as the following equation：

$$MSD(\tau) = \frac{1}{N_m}\sum_{i}^{N_m}\frac{1}{N_\tau}\sum_{t_0}^{N_\tau}[r_i(t_0+\tau) - r_i(t_0)]^2 \qquad (2)$$

where N_m is the number of gas molecules, N_T is the number of time origins used in calculating the average, and r_i is the coordinate of the i-th molecule. In addition, the slope of the MSD as a function of time determines the self-diffusion coefficient (D_s) which is defined according to the so-called Einstein relation [36].

$$MSD(\tau) = 2nD_s\tau + b \qquad (3)$$

where n is the dimension of frameworks (n = 1 for 1-D diffusion, i.e. along the X, Y, and Z in MFI, as well as in 1-D MTW, TON, AFI and AFI zeolite, n = 3 for MFI and in condensed phase). The diffusion coefficients were obtained by fitting the linear region of MSD using a least-square fit. The D_s values were calculated as the average of 3 dependent MD trajectories.

Acknowledgments

This work is supported by the National Natural Science Foundation of China (No. 22032005, 21802164, 21902180, 21991092, 21991090, 22002174 and 91645112), and Natural Science Foundation of Hubei Province of China (2018CFA009), Key Research Program of Frontier Sciences, CAS (No. QYZDB-SSW-SLH026), and Sinopec Corp. (417012-4). The authors are grateful to Shenzhen Cloud Computing Center for their support in computing facilities.

References

[1] A. B. J. Caro, J. K. G. Vogl, and Editors, Diffusive Spreading in Nature. Technology and Society, (2007).

[2] P. Cnudde, R. Demuynck, S. Vandenbrande, M. Waroquier, G. Sastre, and V. Van Speybroeck, Light Olefin Diffusion During the Mto Process on H-Sapo-34: A Complex Interplay of Molecular Factors, J. Am. Chem. Soc. 142, 6007-6017 (2020).

[3] C. Gu, N. Hosono, J. J. Zheng, Y. Sato, S. Kusaka, S. Sakaki, and S. Kitagawa, Design and Control of Gas Diffusion Process in a Nanoporous Soft Crystal. Science 363, 387-391 (2019).

[4] P. J. Bereciartua *et al.*, Control of Zeolite Framework Flexibility and Pore Topology for Separation of Ethane and Ethylene. Science 358, 1068-1071 (2017).

[5] B. Smit and T. L. M. Maesen, Molecular Simulations of zeolite: Adsorption, Diffusion, and Shape Selectivity. Chem. Rev. 108, 4125-4184 (2008).

[6] K. Hahn, J. Karger, and V. Kukla, Single-File Diffusion Observation. Phys. Rev. Lett. 76, 2762-2765 (1996).

[7] V. Gupta, S. S. Nivarthi, D. Keffer, A. V. McCormick, and H. T. Davis, Evidence of Single-File Diffusion in zeolite. Science 274, 164-164 (1996).

[8] V. Kukla, J. Kornatowski, D. Demuth, I. Gimus, H. Pfeifer, L. V. C. Rees, S. Schunk, K. K. Unger, and J. Karger, Nmr Studies of Single-File Diffusion in Unidimensional Channel zeolite. Science 272, 702-704 (1996).

[9] Q. H. Wei, C. Bechinger, and P. Leiderer, Single-File Diffusion of Colloids in One-Dimensional Channels. Science 287, 625-627 (2000).

[10] P. K. Ghorai, S. Yashonath, P. Demontis, and G. B. Suffritti, Diffusion Anomaly as a Function of Molecular Length of Linear Molecules: Levitation Effect. J. Am. Chem. Soc. 125, 7116-7123 (2003).

[11] S. Nag, G. Ananthakrishna, P. K. Maiti, and S. Yashonath, Separating Hydrocarbon Mixtures by Driving the Components in Opposite Directions: High Degree of Separation Factor and Energy Efficiency. Phys. Rev. Lett. 124, 255901(1-6) (2020).

[12] D. Dubbeldam, S. Calero, T. L. M. Maesen, and B. Smit, Incommensurate Diffusion in Confined Systems. Phys. Rev. Lett. 90, 245901(1-4) (2003).

[13] R. L. Gorring, Diffusion of Normal Paraffins in Zeolite-T - Occurrence of Window Effect. J. Catal. 31, 13-17 (1973).

[14] E. G. Derouane and Z. Gabelica, A Novel Effect of Shape Selectivity - Molecular Traffic Control in Zeolite Zsm-5. J. Catal. 65, 486-489 (1980).

[15] E. Ruckenstein and P. S. Lee, Resonant Diffusion. Phys. Lett. A 56, 423-424 (1976).

[16] R. C. Runnebaum and E. J. Maginn, Molecular Dynamics Simulations of alkane in the Zeolite Silicalite: Evidence for Resonant Diffusion Effects. J. Phys. Chem. B 101, 6394-6408 (1997).

[17] D. Dubbeldam, S. Calero, T. L. M. Maesen, and B. Smit, Understanding the Window Effect in Zeolite Catalysis. Angew. Chem. Int. Ed. 42, 3624-3626 (2003).

[18] D. Dubbeldam, E. Beerdsen, S. Calero, and B. Smit, Molecular Path Control in Zeolite Membranes. P. Natl. Acad. Sci. USA 102, 12317-12320 (2005).

[19] S. Gao, Z. Liu, S. Xu, A. Zheng, P. Wu, B. Li, X. Yuan, Y. Wei, and Z. Liu, Cavity-Controlled Diffusion in 8-Membered Ring Molecular Sieve Catalysts for Shape Selective Strategy. J. Catal. 377, 51-62 (2019).

[20] J. Kärger, H. Pfeifer, F. Stallmach, N.N. Feoktistova and S.P. Zhdanov, ^{129}Xe and ^{13}C PFG n.m.r. study of the intracrystalline self-diffusion of Xe, CO_2, and CO. zeolite 13, 50-55 (1993).

[21] A. Ghysels, S. L. C. Moors, K. Hemelsoet, K. De Wispelaere, M. Waroquier, G. Sastre, and V. Van Speybroeck, Shape-Selective Diffusion of Olefins in 8-Ring Solid Acid Microporous zeolite. J. Phys. Chem. C 119, 23721-23734 (2015).

[22] E. Beerdsen, B. Smit, Diffusion in Confinement: Agreement between Experiments Better than Expected. J. Phys. Chem. B 110, 14529-14530(2006).

[23] D. Y. Zhong, J. H. Franke, S. K. Podiyanachari, T. Blomker, H. M. Zhang, G. Kehr, G. Erker, H. Fuchs, and L. F. Chi, Linear Alkane Polymerization on a Gold Surface. Science 334, 213-216 (2011).

[24] H. Jobic, W. Schmidt, C. B. Krause, and J. Karger, Pfg Nmr and Qens Diffusion Study of N-Alkane Homologues in Mfi-Type zeolite. Microporous Mesoporous Mater. 90, 299-306 (2006).

[25] H. Jobic, Diffusion of Linear and Branched alkane in Zsm-5. A Quasi-Elastic Neutron Scattering Study. J Mol Catal a-Chem 158, 135-142 (2000).

[26] F. Leroy and B. Rousseau, Self-Diffusion of N-alkane in Mfi Type Zeolite Using Molecular Dynamics Simulations with an Anisotropic United Atom (Aua) Forcefield. Mol Simulat 30, 617-620 (2004).

[27] K. Hahn and J. Karger, Molecular Dynamics Simulation of Single-File Systems. J. Phys. Chem. 100, 316-326 (1996).

[28] W. Li, M. M. Quesada- Moreno, P. Pinacho and M. Schnell, Unlocking the Water Trimer Loop: Isotopic Study of Benzophenone-(H2O)1-3 Clusters with Rotational Spectroscopy. Angew. Chem. Int. Edit. DOI:10.1002/ange.202013899.

[29] C. Baerlocher, L. B. McCusker, Database of Zeolite Structures. http://www.iza structure.org/databases/ (Accessed Jun 2016).

[30] J. D. Gale, A. L. Rohl, The General Utility Lattice Program (Gulp). Mol Simulat 29, 291-341 (2003).

[31] C. R. A. Catlow, C. M. Freeman, B. Vessal, S. M. Tomlinson and M. Leslie, Molecular-Dynamics Studies of Hydrocarbon Diffusion in zeolite. J. Chem. Soc., Faraday Trans. 87, 1947-1950 (1991).

[32] M. J. Sanders, M. Leslie, C. R. A. Catlow, Interatomic Potentials for Sio_2. J. Chem. Soc. Chem. Comm. 1271-1273 (1984).

[33] P. Bai, M. Tsapatsis and J. I. Siepmann, Trappe-Zeo: Transferable Potentials for Phase Equilibria Force Field for All-Silica zeolite. J. Phys. Chem. C 117, 24375-24387 (2013).

]34] C. D. Wick, M. G. Martin and J. I. Siepmann, Transferable Potentials for Phase Equilibria. 4. United-Atom Description of Linear and Branched Alkenes and Alkylbenzenes. J. Phys. Chem. B 104, 8008-8016 (2000).

[35] W. Smith, T. R. Forester, Dl_Poly_2.0: A General-Purpose Parallel Molecular Dynamics Simulation Package. J. Mol. Graph. 14, 136-141 (1996).

[36] D. Frenkel, B. Smit, Understanding Molecular Simulations (Elsevier, Singapore, 2002).